MATERIALS AND METHODS

Cloning of newt *B4* cDNA

Total RNA was extracted from *Cynops pyrrhogaster* ovary using TRIzol reagent (Invitrogen, Carlsbad, CA, USA), and poly(A) RNA was purified using oligotex-dT30 (Takara, Ohtsu, Japan). Ovary cDNA library was constructed using Universal RiboClone cDNA synthesis system (Promega, Madison, WI, USA). In this procedure, RT reaction was performed using random hexameric primers and cDNA was inserted into the EcoRV site in pBluescript SK(+). Using the ovary cDNA library, 4582 expressed sequence tags were obtained, and 2 clones showed a similarity with frog oocyte-type linker histone. 5′- and 3′-rapid amplification of cDNA ends RACE) was performed, and finally full-length *C. pyrrhogaster B4* clone was obtained by end-to-end (from the initial methionine to stop codon) PCR. A partial sequence of *Notophthalmus viridescens B4* was obtained from ovary by RT-PCR using primers based on the *C. pyrrhogaster B4* sequence. 5′-and 3′-RACE was performed, and full-length *N. viridescens B4* was cloned by end-to-end PCR (Supplemental Fig. 1).

Accession number of cloned cDNAs

Full or partial cDNAs were cloned by degenerate PCR and rapid amplification of cDNA ends. Accession numbers of cloned cDNAs are GQ890215 (*C. pyrrhogaster B4*), GQ890216 (*N. viridescens B4*), GQ844313 (*N. viridescens nucleostemin*), GQ844312 (*N. viridescens MafB*), GQ844314 (*N. viridescens* γ*-crystallin*), and GQ844315 (*N. viridescens* β*-actin*).

RT-PCR

Dorsal irises during lens regeneration were collected. RNAs were extracted using Trizol reagent (Invitrogen) for *C. pyrrhogaster* or Nucleospin (Macherey-Nagel, Düren, Germany) for *N. viridescens*. RT reaction was performed with a first-strand cDNA synthesis kit (GE Healthcare, Piscataway, NJ, USA) using an oligo(dT) primer. PCR for B4 was performed using the Ex *Taq* kit (Takara) and the following primers, *Cynops*-B4-RT-PCR-F, 5′-ATGGTACTGGAAGCCCTGAGG-3′; *Cynops*-B4-RT-PCR-R, 5′-ACGGAGTCCACAGACGGGTA-3′; *Notophthalmus*-B4-RT-PCR-F, 5′-GGCCACAGGAAGGTTTAAGCT-3′; *Notophthalmus*-B4-RT-PCR-R, 5′-CTCGACACCACTTTCTTGGCT-3′; *Cynops*-actin-RT-PCR-F, 5′-GAAGGTTATGCCCTGCCTCAT-3′; *Cynops*-actin-RT-PCR-R, 5′-TGAAGCTGTAGCCCCTCTCAGT-3′; *Notophthalmus*-actin-RT-PCR-F, 5′- TTATGCTCTGCCTCATGCCATCCT-3′; *Notophthalmus*-actin-RT-PCR-R, 5′- TTCGGCCGTAGTTGTGAAGCTGTA-3′.

Quantitative PCR

Regenerated lenses were collected using a mouth pipette. RNA was purified using Nucleospin (Macherey-Nagel). RT reaction was performed with a first-strand cDNA synthesis kit (GE Healthcare) using an oligo(dT) primer. qPCR was performed using a iQ SYBR Green supermix (Bio-Rad, Hercules, CA, USA), and the following primers: nucleostemin-qPCR-F, 5′-ATCTGCGGCCAAGAAAGAAACTGC-3′; nucleostemin-qPCR-R 5′-ATGTTTATCAGGAGCCTGGTCGGT-3′; MafB-qPCR-F, 5′-TGGACGCTCTAATCAACTCTGCCA-3′; MafB-qPCR-R; 5′-TTAGCAAGTAGCCTGGGTGCGTAT-3′; Pax6-qPCR-F, 5′-ATCGGAGGCAGCAAGCCCA-3′; Pax6-qPCR-R, 5′-AGATGGACGGACACTCGCGCTT-3′; γ-crystallin-qPCR-F, 5′-AATGATTCCATCAGGTCATGCCGC-3′; γ-crystallin-qPCR-R, 5′-TGTGGACAGTCTTCAGAGAACTCC-3′; RPL27-qPCR-F, 5′-ATTTATGAAACCCGGGAAGG-3′; RPL27-qPCR-R, 5′-CCAGGGCATGACTGTAAGGT-3′. To quantitate the expression of each gene, C_t values were compared to a standard curve generated using a series of dilutions of cloned cDNAs. The amount of mRNA was normalized to that of ribosomal protein L27. Specific PCR amplifications were confirmed by melting curve analysis.

Vivo-morpholino

Vivo-morpholinos specialized to enter cells in living animals were purchased from Gene Tools (Philomath, OR, USA). After lentectomy, B4 vivo-morpholino (5′-AGCAGTCTTCTTAGAAGCCATTTG-3′) or the control vivo-morpholino recommended by Gene Tools (5′-CCTCTTACCTCAGTTACAATTTATA-3′) was intraperitoneally injected at 12.5 μg/g body weight every day until different samples were collected.

Antibodies

Rabbit polyclonal antibody against newt B4 was raised against a mixture of two peptides, ALRKNTDRKGAT and TDKDSAKPTAKRGKK (see Supplemental Fig. 1A) and affinity-purified using the peptides (Scrum Inc., Tokyo, Japan). The other primary antibodies used were histone H1 (V7013; Biomeda, South San Francisco, CA, USA), histone H3 (ab1791; Abcam, Cambridge, UK), and BrdU (MAB3510; Millipore, Billerica, MA, USA).

Immunohistochemistry

Eyeballs and ovaries were fixed with methanol-acetic acid solution (75% methanol and 25% acetic acid, v/v) at 4°C overnight, embedded in paraffin, and sectioned at 16 μm. After deparaffinization, sections were treated with permeable solution (0.05% Triton X-100, 0.05% saponin, and 2× SSC) for 1 h, rinsed with 2× SSC, and blocked in TNB buffer (0.1 M Tris-HCl, pH7.5; 0.15 M NaCl; and 0.5% blocking reagent) supplied with the TSA kit (Perkin Elmer, Waltham, MA, USA) for 1 h.

For detection of B4 and histone H1, the samples were incubated at 4°C overnight with a mixture of the primary antibodies, B4 antibody diluted 1:10 and histone H1 antibody diluted 1:100 with TNB buffer, and then incubated with the following secondary antibodies at room temperature for 90 min: Alexa Fluor 488-conjugated goat anti-rabbit IgG for B4 and Cy3-conjugated sheep anti-mouse IgG for histone H1. Nuclei were counterstained with Hoechst 33258. Images of stained tissue were taken using the BX-51 fluorescence microscope system (Olympus, Tokyo, Japan) equipped with a Cool SNAP cf2 camera (Photometrics, Tucson, AZ, USA). All images taken were saved in TIFF format. For measurement of signal intensity, the average signal intensity per pixel of B4, histone H1, and Hoechst33258 in each nucleus was measured using MetaMorph 7.1 software (Molecular Devices, Sunnyvale, CA, USA) without any image processing.

For BrdU staining, the samples were incubated at 4°C overnight with BrdU antibody diluted 1:100 with TNB buffer and then incubated with Alexa Fluor 488-conjugated goat anti-mouse IgG at room temperature for 90 min. To detect apoptotic cells, ApopTag Plus In Situ Apoptosis Fluorescein Detection kit (Millipore) was used according to the manufacturer's instruction.

Western blot analysis

Tissues were homogenized in 10 vol of 70% PBS. Two volumes of 0.6N HCl (final 0.2 N) was added to the homog-

enate and kept on ice 30 min to extract histones. The supernatant was recovered after centrifugation at 10,000 g for 10 min at 4°C and dialyzed twice with 0.1 N acetic acid for 30 min and twice with milli Q water for 30 min, followed by overnight incubation at 4°C. The extracted proteins were separated by SDS-PAGE and blotted onto a nitrocellulose membrane (0.2 μm pore size, Invitrogen). The B4 band was probed with anti-B4 antibody followed by alkaline phosphatase-conjugated anti-rabbit IgG (Abcam). The histone H3 band was probed with anti-histone H3 antibody followed by alkaline phosphatase-conjugated anti-rabbit IgG (Abcam). The bands were visualized by incubation with NBT/BCIP solution (Roche, Basel, Switzerland). Intensity of the detected bands was measured using ImageJ 1.40g software (U.S. National Institutes of Health, Bethesda, MD, USA). The amount of each histone in B4 morpholino-treated iris sample was calibrated using a standard curve generated by dilutions of control morpholino-treated iris sample. The amount of B4 protein was normalized to that of histone H3.

Animal study compliance

All animal care and use protocols were in compliance with the Animal Experiment Handbook at the Kobe Center for Developmental Biology (RIKEN Kobe) and the U.S. Department of Health and Human Services Guide for the Care and Use of Laboratory Animals.

RESULTS

Expression of B4 during Newt lens regeneration

Initial immunohistochemical analysis using a *Xenopus* oocyte-type linker histone B4 antibody showed that antigens reacting with the antibody accumulate in nuclei of PECs during newt lens regeneration. This finding prompted us to clone a full-length *B4* cDNA from two newt species, *C. pyrrhogaster* and *N. viridescens* (Supplemental Fig. 1). RT-PCR experiments clearly indicated that B4 is expressed during lens regeneration in both species (**Fig. 1***A*). Antibody specific for newt B4 was raised using a mixture of newt B4 peptide sequences as antigens. Western blot analysis using this antibody also indicated that B4 is expressed during newt lens regeneration (Fig. 1*B, C*).

Nuclear recruitment of B4 during lens regeneration

Having established the presence of B4 during regeneration, we decided to follow expression of B4 and H1 throughout a period of 20 d after lentectomy. The results are shown in **Fig. 2**. In ovaries, B4 localizes in the germinal vesicle, while H1 localizes in nucleus of follicle cells (Fig. 2*A*). In intact iris (d 0), B4 is virtually absent, while H1 is present in PECs. On d 8, when dedifferentiation is ongoing, PECs are positive for both B4 and H1. Similar patterns were observed at d 12 (Fig. 2*B*). A clear pattern emerged when we quantitated the expression and plotted the ratio of B4 to H1 (see Materials and Methods). Starting at d 8, the ratio of B4 to H1 clearly increases in the dorsal iris vesicle. Then, this ratio reaches a peak at d 12

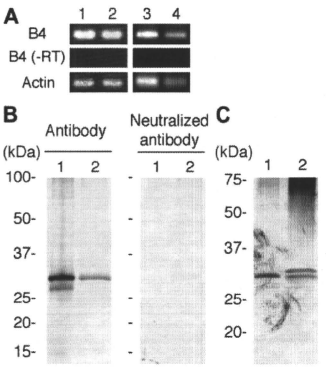

Figure 1. Expression of B4 during lens regeneration. *A*) Detection of *B4* expression by RT-PCR. Lane 1, *C. pyrrhogaster* ovary; lane 2, *C. pyrrhogaster* dorsal iris 10 d after lentectomy; lane 3, *N. viridescens* ovary; lane 4, *N. viridescens* dorsal iris 10 d after lentectomy. *B, C*) Detection of B4 protein by Western blot analysis. Ovary (lane 1) and dorsal iris 10 d after lentectomy (lane 2) were collected from *C. pyrrhogaster* (*B*) or *N. viridescens* (*C*), and histone proteins were extracted. Extracted proteins were analyzed by Western blotting using B4 peptide antibody (*B*, left panel). To confirm specific detection of B4 protein, the antibody was neutralized by incubation with antigen peptides prior to the primary antibody reaction (*B*, right panel). Note that the neutralizing antibody abolished bands indicating specificity of the antibody. Note that two bands, one band showing same mobility with the band detected in ovary and another band showing slightly less mobility, were detected in *N. viridescens* lens regenerating iris (*C*), which suggests alternative splicing or post-translational modifications of B4 in the iris.

before lens differentiation begins. Finally, it declines by d 18, when the transdifferentiation process is completed and what continues is the growth of the lens (Fig. 2*C*). Such a peak of the ratio is not seen in the ventral iris.

B4 knockdown affects proliferation and apoptosis

These striking patterns of B4 recruitment prompted us to examine its role in more details. For this, we proceeded by knocking down expression of B4, employing vivo-morpholino technology (19). To assess whether B4 morpholino reduces expression of B4, we injected morpholino every day intraperitonealy for 10 d after lentectomy. Then, dorsal irises were collected, and linker and core histones were extracted with hydrochloric acid. The extracted histones were analyzed by Western blotting. The amount of B4 was calculated based on the intensity of the detected band and normalized with that of histone H3. In irises from newts treated with the B4 morpholino, the amount of B4 protein was decreased by nearly 50% when compared to the levels in irises from newts injected with control morpholino (**Fig. 3***A*).

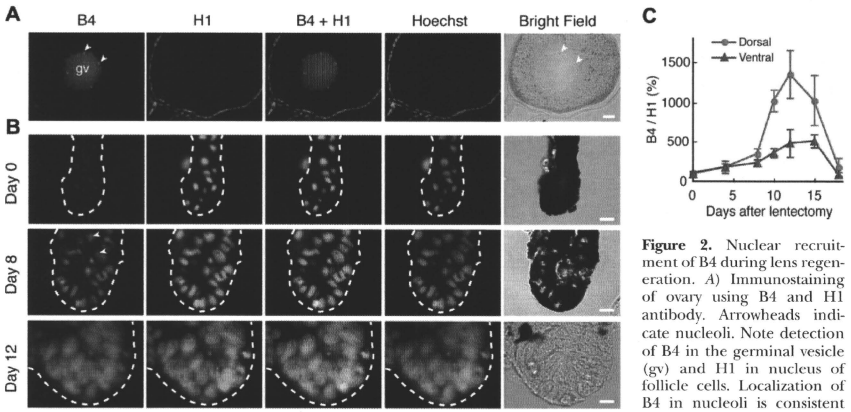

Figure 2. Nuclear recruitment of B4 during lens regeneration. *A*) Immunostaining of ovary using B4 and H1 antibody. Arrowheads indicate nucleoli. Note detection of B4 in the germinal vesicle (gv) and H1 in nucleus of follicle cells. Localization of B4 in nucleoli is consistent with previous observations in mice (7, 18). *B*) Immunostaining during lens regeneration (0, 8, and 12 d after lentectomy) using B4 and H1 antibodies. Note that B4 is scarcely detected in intact iris. Note that the staining intensities of each panel are not comparative, because images were processed independently in order to show nuclear distribution of each antigen. *C*) Changes in the ratio of B4 to histone H1 during lens regeneration. After immunostaining, the intensity of B4 and H1 signals in each nucleus were measured, and the ratio of B4 to histone H1 was calibrated. Error bars = SD. Scale bars = 200 μm (*A*), 20 μm (*B*).

Following such a positive outcome of the morpholino treatment, we conducted a large-scale experiment by injecting morpholino and examining the regenerating lens for a period up to 20 d. We started seeing effects on lens differentiation and morphology after d 12, which correlated well with the expression and recruitment of B4. By d 20, we could conclude that the regenerated lens was considerably smaller in B4 morpholino-treated newts (Fig. 3*B*, *E*, *F*). On d 20, the lens size of B4 morpholino-injected newts was nearly half that of the control morpholino-injected newts (Fig. 3*B*). To investigate how B4 mediates such an effect on lens differentiation, we studied levels of cell proliferation and apoptosis in the regenerating lenses. BrdU was administered 24 h before fixation at different times, and its incorporation was analyzed by immunostaining. As expected, in control morpholino-injected newts the percentage of BrdU-positive cells was increased after 12 d. However, this percentage was significantly decreased in B4 morpholino-injected newts on d 16 and 20 (Fig. 3*C*, *E*). Next, Tunel staining was performed to examine whether lack of B4 leads to cell death. Indeed, it was shown that on d 20 significantly higher numbers of cells were undergoing apoptosis due to B4 morpholino treatment (Fig. 3*D*, *F*). Thus, so far our results clearly indicate an association between expression of B4 and lens transdifferentiation, which leads to a structurally normal lens. The reader should bear in mind that complete loss of B4 cannot result from the morpholino treatment; thus, even 50% decline in expression could elicit these results.

B4 is required for lens-specific gene expression during transdifferentiation

Despite the fact that the smaller lenses in B4 morpholino-injected newts can be attributed to an effect on proliferation and apoptosis, it is imperative to show whether expression of key genes known to regulate lens regeneration is affected by the B4 morpholino treatment. To examine this, we again injected newts for 20 d with B4 morpholino, collected only the regenerated lenses, isolated RNA, and examined the levels of several genes that are known to be structural and regulatory markers in lens differentiation and regeneration by qPCR. The expression of each gene was normalized with that encoding for ribosomal protein L27 so that we could account for the effect on lens size. Interestingly, we observed a dramatic down-regulation of γ-crystallin to 4% in regenerated lens from B4 morpholino-treated newts when compared to control. Likewise, we observed down-regulation of MafB and Pax-6, both known transcriptional factors that bind crystallin gene promoters (20, 21). On the contrary, we show up-regulation of nucleostemin (**Fig. 4**). Nucleostemin, a nucleolar protein that has been found in stem cells and cancer cells (22), is expressed in PECs during dedifferentiation and disappears after lens differentiation (23). Thus, it seems that the lens in B4 morpholino-treated animals retains the status of an earlier stage. From the effect of B4 knockdown on gene expression, it is clear that B4 is required for lens-specific gene expression during transdifferentiation.

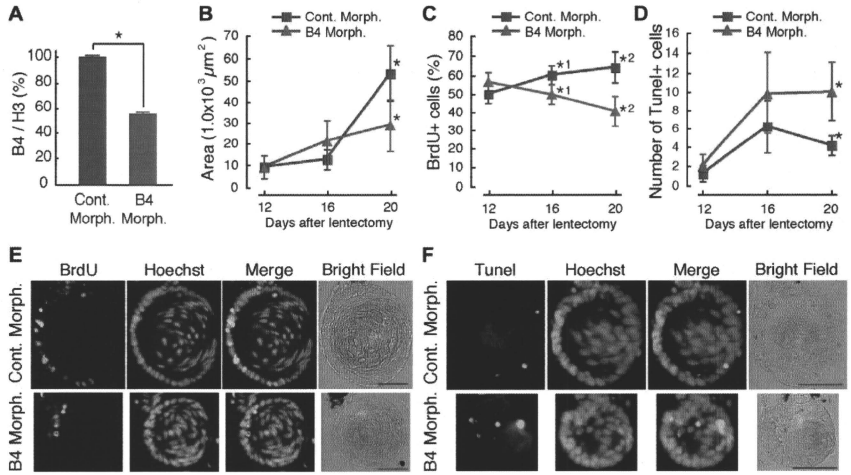

Figure 3. B4 knockdown affects proliferation and apoptosis. *A*) Decrease of B4 protein after B4 morpholino injection. After lentectomy, B4 vivo-morpholino was injected intraperitoneally every day in *N. viridescens*. On d 10, dorsal irises were collected, and the amount of B4 protein in the irises was measured by Western blotting. Amount of B4 was normalized with that of histone H3. $*P = 0.000310$ (control, $n=2$; B4, $n=2$). *B–F*) Effect of B4 knockdown in lens regeneration. *B*) Size of regenerated lens. $*P = 0.00262$ (control, $n=7$; B4, $n=9$). *C*) Number of BrdU-positive cells. *1: $P = 0.0176$ (control, $n=4$; B4, $n=7$); *2: $P = 0.0000972$ (control, $n=7$; B4, $n=10$). *D*) Number of Tunel-positive cells. $*P = 0.00738$ (control, $n=6$; B4, $n=6$). Error bars = SD. *P* values are from Student's *t* test (2-tailed). *E*) BrdU immunostaining of lens from morpholino-injected newts 20 d after lentectomy. *F*) Tunel staining of lens from morpholino-injected newts 20 d after lentectomy. Scale bars = 100 μm. Cont. Morph., control vivo-morpholino; B4 Morph., B4 vivo-morpholino.

DISCUSSION

Transdifferentiation of PECs in newt lens regeneration is one of most obvious examples of *in vivo* reprogramming of somatic cells. It is also known that nuclear reprogramming is induced artificially by somatic cell nuclear transfer (SCNT) into oocytes, where genome-wide chromatin decondensation is mediated by replacement of linker histone H1 with histone B4. We hypothesized that similar events to SCNT might occur during reprogramming of PECs to lens cells. To test this hypothesis, we first cloned and examined expression of B4 during the process of lens regeneration. Indeed, we show that B4 is expressed in newt somatic cells. This is the first time that B4 was found in somatic cells. All previous studies in many animals, including mice, zebrafish, frogs, and sea urchins, have shown that B4 is specific to oocyte and early embryo before the onset of zygotic gene expression (7–12).

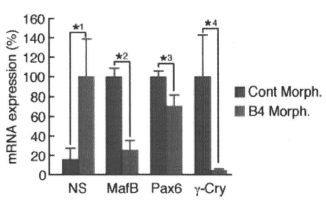

Figure 4. B4 is required for lens-specific gene expression during transdifferentiaion. Effects of B4 knockdown on gene expression were analyzed by qPCR. Clear indications show that B4 knockdown significantly down-regulates lens differentiation-specific markers, such as MafB, Prox1, and γ-crystallin (γ-Cry). However, nucleostemin (NS), a nucleolar protein related to stem cell-like state, is up-regulated. Error bars = SD. *P* values are from Student's *t* test (2-tailed). *1: $P = 0.0350$ ($n=4$); *2: $P = 0.0000249$ ($n=4$); *3: $P = 0.00342$ ($n=4$); *4: $P = 0.0298$ ($n=4$). Cont. Morph., control vivo-morpholino; B4 Morph., B4 vivo-morpholino.

In addition to showing expression of B4 in PECs, we have also demonstrated that B4 has a function during lens transdifferentiation. Knocking down B4 induces apoptosis and negatively affects cell proliferation and lens differentiation, as shown by morphological as well as molecular criteria. Notably, we found that B4 regulates expression of key transcriptional factors, such as pax-6 and MafB, and of lens differentiation specific markers, such as γ-crystallin. However, knockdown of B4 up-regulates nucleostemin, a stem cell-specific marker, which is expressed during PEC dedifferentiation. However, the exact mechanisms whereby B4 acts on lens regeneration remain unclear. Nevertheless, we can offer two possible models. One is nonselective

replacement. According to this, B4 would replace H1 nonselectively. This replacement would cause genome-wide chromatin decondensation similar to the reprogramming mediated by SCNT (16, 17). Such chromatin decondensation might allow transcriptional factors to interact with the promoter region of lens differentiation genes. The other model is selective replacement. In this case, B4 would affect expression of specific factors that need to interact with H1 for regulation. An example of such regulation has been shown in the case where Msx1 cooperates with H1b for repression of MyoD to inhibit muscle differentiation (24). To address those hypotheses, we need genome-wide ChIP-on-chip analysis. Such an experiment is not possible at present because the newt genome has not been sequenced.

Collectively, our expression and functional experiments identified a novel role of the linker histone B4. This is the first time that this oocyte-specific linker histone, which has been associated with reprogramming, was found to be expressed in adult somatic cells and, moreover, controls the process of transdifferentiation and lens regeneration. This finding suggests that reprogramming in germ cells and regenerating newt cells share similar strategies, thus providing a novel paradigm about cellular plasticity. In this case our results open new avenues for experimentation in regenerative biology. FJ

The authors thank Y. Tanabe, and J. Hayashi for EST analysis. The authors are grateful to K. Ura for a helpful discussion. This work was supported by a KAKENHI grant (17657068) to N.M.; by the Naito Foundation and the Project for Realization of Regenerative Medicine as well as a Grant-in-Aid for Creative Research from the Japan Ministry of Education, Culture, Sports, Science, and Technology (17GS0318) to K.A., and by a U.S. National Institutes of Health grant (EY10540) to P.A.T.

REFERENCES

1. Abe, S., and Eguchi, G. (1977) An analysis of differentiative capacity of pigmented epithelial cells of adult newt iris in clonal cell culture. *Dev. Growth Differ.* **19,** 309–317
2. Eguchi, G., and Okada, T. S. (1973) Differentiation of lens tissue from the progeny of chick retinal pigment cells cultured in vitro: a demonstration of a switch of cell types in clonal cell culture. *Proc. Natl. Acad. Sci. U. S. A.* **70,** 1495–1499
3. Li, E. (2002) Chromatin modification and epigenetic reprogramming in mammalian development. *Nat. Rev. Genet.* **3,** 662–673
4. Martin, C., and Zhang, Y. (2005) The diverse functions of histone lysine methylation. *Nat. Rev. Mol. Cell. Biol.* **6,** 838–849
5. Neelin, J. M., Callahan, P. X., Lamb, D. C., and Murray, K. (1964) The histones of chicken erythrocyte nuclei. *Can. J. Biochem. Physiol.* **42,** 1743–1752
6. Godde, J. S., and Ura, K. (2009) Dynamic alterations of linker histone variants during development. *Int. J. Dev. Biol.* **53,** 215–224
7. Tanaka, M., Hennebold, J. D., Macfarlane, J., and Adashi, E. Y. (2001) A mammalian oocyte-specific linker histone gene H1oo: homology with the genes for the oocyte-specific cleavage stage histone (cs-H1) of sea urchin and the B4/H1M histone of the frog. *Development* **128,** 655–664
8. Cho, H., and Wolffe, A. P. (1994) Xenopus laevis B4, an intron-containing oocyte-specific linker histone-encoding gene. *Gene* **143,** 233–238
9. Mandl, B., Brandt, W. F., Superti-Furga, G., Graninger, P. G., Birnstiel, M. L., and Busslinger, M. (1997) The five cleavage-stage (CS) histones of the sea urchin are encoded by a maternally expressed family of replacement histone genes: functional equivalence of the CS H1 and frog H1M (B4) proteins. *Mol. Cell. Biol.* **17,** 1189–1200
10. McGraw, S., Vigneault, C., Tremblay, K., and Sirard, M. A. (2006) Characterization of linker histone H1FOO during bovine in vitro embryo development. *Mol. Reprod. Dev.* **73,** 692–699
11. Wibrand, K., and Olsen, L. C. (2002) Linker histone H1M transcripts mark the developing germ line in zebrafish. *Mech. Dev.* **117,** 249–252
12. Muller, K., Thisse, C., Thisse, B., and Raz, E. (2002) Expression of a linker histone-like gene in the primordial germ cells in zebrafish. *Mech. Dev.* **117,** 253–257
13. Teranishi, T., Tanaka, M., Kimoto, S., Ono, Y., Miyakoshi, K., Kono, T., and Yoshimura, Y. (2004) Rapid replacement of somatic linker histones with the oocyte-specific linker histone H1foo in nuclear transfer. *Dev. Biol.* **266,** 76–86
14. Gao, S., Chung, Y. G., Parseghian, M. H., King, G. J., Adashi, E. Y., and Latham, K. E. (2004) Rapid H1 linker histone transitions following fertilization or somatic cell nuclear transfer: evidence for a uniform developmental program in mice. *Dev. Biol.* **266,** 62–75
15. Becker, M., Becker, A., Miyara, F., Han, Z., Kihara, M., Brown, D. T., Hager, G. L., Latham, K., Adashi, E. Y., and Misteli, T. (2005) Differential in vivo binding dynamics of somatic and oocyte-specific linker histones in oocytes and during ES cell nuclear transfer. *Mol. Biol. Cell* **16,** 3887–3895
16. Saeki, H., Ohsumi, K., Aihara, H., Ito, T., Hirose, S., Ura, K., and Kaneda, Y. (2005) Linker histone variants control chromatin dynamics during early embryogenesis. *Proc. Natl. Acad. Sci. U. S. A.* **102,** 5697–5702
17. Wade, P. A., and Kikyo, N. (2002) Chromatin remodeling in nuclear cloning. *Eur. J. Biochem.* **269,** 2284–2287
18. Tanaka, M., Kihara, M., Hennebold, J. D., Eppig, J. J., Viveiros, M. M., Emery, B. R., Carrell, D. T., Kirkman, N. J., Meczekalski, B., Zhou, J., Bondy, C. A., Becker, M., Schultz, R. M., Misteli, T., De La Fuente, R., King, G. J., and Adashi, E. Y. (2005) H1FOO is coupled to the initiation of oocytic growth. *Biol. Reprod.* **72,** 135–142
19. Morcos, P. A., Li, Y., and Jiang, S. (2008) Vivo-Morpholinos: a non-peptide transporter delivers Morpholinos into a wide array of mouse tissues. *BioTechniques* **45,** 613–614. 616, 618
20. Cvekl, A., Kashanchi, F., Sax, C. M., Brady, J. N., and Piatigorsky, J. (1995) Transcriptional regulation of the mouse alpha A-crystallin gene: activation dependent on a cyclic AMP-responsive element (DE1/CRE) and a Pax-6-binding site. *Mol. Cell. Biol.* **15,** 653–660
21. Yoshida, T., and Yasuda, K. (2002) Characterization of the chicken L-Maf, MafB and c-Maf in crystallin gene regulation and lens differentiation. *Genes Cells* **7,** 693–706
22. Tsai, R. Y., and McKay, R. D. (2002) A nucleolar mechanism controlling cell proliferation in stem cells and cancer cells. *Genes Dev.* **16,** 2991–3003
23. Maki, N., Takechi, K., Sano, S., Tarui, H., Sasai, Y., and Agata, K. (2007) Rapid accumulation of nucleostemin in nucleolus during newt regeneration. *Dev. Dyn.* **236,** 941–950
24. Lee, H., Habas, R., and Abate-Shen, C. (2004) MSX1 cooperates with histone H1b for inhibition of transcription and myogenesis. *Science* **304,** 1675–1678

Received for publication April 2, 2010.
Accepted for publication April 29, 2010.

2 血清・血漿バイオマーカー探索のための新しい前処理法の開発

朝長 毅，小寺義男

種々の疾病の診断および創薬のための血清・血漿バイオマーカーの探索は重要であるが，まだ満足のいくバイオマーカーを提案できているとは言い難い．この理由は，血清・血漿中のタンパク質のダイナミックレンジが10^{11}と幅広く，現在のプロテオミクス技術ではその中の量の多いタンパク質しか捉えられていないためと考えられる．疾病特異的なバイオマーカータンパク質はごく微量であり，そのような微量成分を検出する手法の開発，特に9割以上を占めるメジャータンパク質を取り除く効果的な前処理法の開発が急務である．本稿では，最近われわれが独自に開発した血清前処理法を紹介し，疾患バイオマーカータンパク質・ペプチド探索への臨床応用について述べる．

1 用いる解析法と進め方

1）低分子量タンパク質・ペプチドの高効率抽出法（DS法）の開発

創薬のターゲットとなる疾患バイオマーカー探索をプロテオミクス解析で行う場合の流れとして，通常罹患部の組織やモデル動物・細胞を用いて疾患特異的タンパク質を同定し，そのタンパク質の機能解析を通じて，疾患発症との関連を理解し，創薬に結びつけるという方法が一般的である．しかし，血液中には病巣から漏出・分泌されるタンパク質が存在すると考えられるため，そのようなタンパク質を直接プロテオミクス解析で検出・同定することも疾患バイオマーカー探索の1つの手段である．例えば，がんの転移にはその前準備として転移病巣に骨髄細胞が集積することが知られているが，そのメカニズムとして，がんの主病巣からのシグナルによって，転移予定組織から分泌されるタンパク質が原因となっていることが報告されており[1]，そのような液性因子の検出には血清・血漿プロテオミクスが威力を発揮すると思われる．

しかし，血清・血漿を用いたプロテオミクス解析の最大の問題点は，その中に含まれるタンパク質濃度のダイナミックレンジの広さであり，最大量と最小量のタンパク質の濃度比が10^{11}もあることである．血清・血漿中にはアルブミン，免疫グロブリンをはじめとした約20種類の高存在量タンパク質が総タンパク質量の99％を占めていることに加えて，タンパク質濃度のダイナミックレンジは組織，細胞に比べて10^3～10^4大きく，現在のプロテオミクス技術ではそのレンジをカバーすることは到底不可能である[2]．したがって，血清・血漿中の組織由来の情報を含む微量な疾患バイオマーカーを探索するためには，濃度に応じた前処理法が必要不可欠である．現在最もよく用いられている方法は，上述の高存在量タンパク質の除去カラムである．しかし，その除去カラムを用いるだけでは，一部の高濃度タンパク質を除去

概略図　バイオマーカー探索のためのタンパク質・ペプチド比較分析法の実験手順

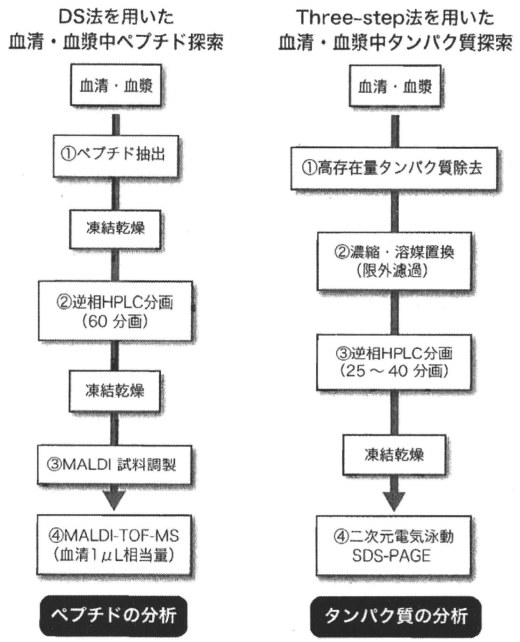

することしかできないため，処理後の血清・血漿のタンパク質濃度のダイナミックレンジは10^9～10^{10}くらいまで低下するにすぎない．近年，除去カラム処理後に多段階のHPLCを用いて分画を行い，微量なタンパク質を検出しようとする試みがなされているが，分画すればするほどその過程におけるタンパク質の損失が大きくなるうえに，スループットや再現性が落ちるという欠点が生じる[3]．血清・血漿分析のもう1つの大きな問題点は，多くのタンパク質・ペプチドがアルブミンなどのキャリアタンパク質に結合して存在しているため，キャリアタンパク質の除去に伴ってこれらの結合タンパク質・ペプチドを損失する点である．特にペプチドにおいては顕著である．

このためわれわれは，①いかにスループットや再現性を維持しながら，微量なタンパク質・ペプチドを検出・同定するか，②アルブミン等のキャリアタンパク質の除去に伴うペプチド成分の損失をいかに減らすことができるかの2点についてさまざまな条件検討を行い，低分子量タンパク質・ペプチドの高効率抽出法〔differential solubilization method（DS法：別名K法）〕の開発に至った[4,5]．一方，このDS法で除去されるタンパク質成分（主に分子量20,000以上）に関しては，市販の高存在量タンパク質除去カラムと逆相HPLC，電気泳動法を組み合わせた再現性の高い比較分析法を採用している（以後，Three-step法と記述する）．**概略図**に，われわれのグループで行っている血清・血漿中のバイオマーカー

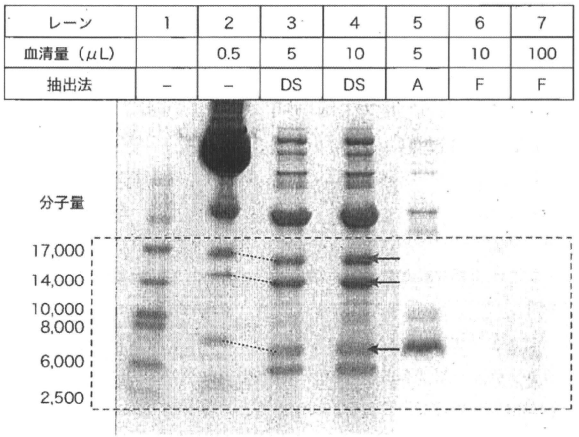

図1　DS法で抽出したペプチドの電気泳動分析結果

レーン1：分子量マーカー，レーン2：未処理血清0.5μL，レーン3，4：血清5μLならびに10μLからDS法で抽出した成分，レーン5：有機溶媒沈殿法（A）で血清5μLから抽出した成分，レーン6，7：限外濾過法（F）で血清10μLならびに100μLから抽出した成分（文献4より転載）

タンパク質・ペプチドの探索までの流れを示す．

2）DS法の原理

低分子量タンパク質・ペプチドを対象としたDS法の原理はまず，1）高濃度のアセトンに血清を混ぜることにより，すべてのタンパク質，ペプチドを沈殿させる．その後，2）タンパク質と低分子量タンパク質・ペプチドの溶解度の違いを利用して，70％アセトニトリルにより，低分子量タンパク質・ペプチドだけを溶解して回収する．従来，血清の前処理によく用いられている高存在量タンパク質除去カラムや有機溶媒沈殿法では，アルブミン等のキャリアタンパク質の除去に伴いペプチド成分が大きく損失する．これに対して，DS法では，1）の過程において，血清中のタンパク質・ペプチドを変性させてアセトンで沈殿させることによって，アルブミンに結合したペプチドを比較的高効率に回収することを可能としている（図1，詳しくは後述）．一方，タンパク質を対象としたThree-step法はクラシカルな方法ではあるが，各ステップのタンパク質の損失を極力抑え，かつ，再現性を高めることにより，探索感度および比較分析精度の向上をめざしている．質量分析計に依存した高感度化は，しばしば結果の不安定性を導く．したがって，いずれの場合も，前処理の高効率化，つまり目的物の損失を抑えて不要な物の除去効率を上げることによって，質量分析計への負担を少なくすることが再現性の高い比較分析には重要であると考えている．

2　研究のプランニング

1）DS法をもとにしたペプチド探索の流れ

DS法を基盤にしたマーカー候補ペプチド探索の研究プランニングは以下のとおりである（**概略図左**）．

①血清10μLを対象に，DS法にてペプチドを抽

出．その後，凍結乾燥にて濃縮し，使用まで保存．

②①をH_2O/0.1％TFA（トリフルオロ酢酸）で溶解し，逆相HPLCでペプチドを60分画に分画．

③②の各分画物をH_2O/0.1％TFA 10 μLで溶かして，そのうちの1 μLをマトリクス試薬と混ぜてMALDI plateにて乾固．

④③をMALDI-TOF-MS測定．

通常はコントロール群と疾患群8血清ずつ（計16血清）を一度にDS処理し，②，③を経てMALDI-TOF-MS分析を行う．比較分析のためには，①はもとより②，③の再現性が非常に重要である．この点に関しては，②のHPLC分画は連続で行うこと，④のMALDI-TOF-MS測定は血清ごとに行うのではなく，16血清の同一分画について同時に③，④を行うことにしている．また，MALDI-TOF-MS測定においては，最も強度の大きいピークを飽和させないレーザー強度で一定回数測定し，ノイズレベルを合わせて比較解析し，疾患特異的に変動するピークを探索している．同一血清を10 μLずつ4～8サンプルに分けて①～④の過程を行い，各ステップの再現性を確認することをお勧めする（**図2**に同一血清を6つに分けて分析した結果を示す．詳しくは後述）．われわれはこの比較方法により，10 μLという微量の血清から数ng/mL以下の微量疾患関連ペプチドの検出に成功している．

高効率なペプチド抽出法を使うことの波及効果は，存在量の少ない微量な疾患関連ペプチドの探索が可能な点，スケールアップによりペプチドの正確な同定が容易である点，幅広い臨床検査の前処理法として応用が可能である点，患者への負担が少ない点など，すべての面において有利な点が多い．

2）Three-step法によるタンパク質探索の流れ

Three-step法によるマーカー候補タンパク質探索の研究プランニングは以下のとおりである（**概略図右**）．

①市販の高存在量タンパク質除去カラムを用いて高存在量タンパク質を除去．

②①を限外濾過フィルターを用いて濃縮するとともに，逆相HPLC用の溶媒（H_2O/0.1％TFA）に置換．

＊①の処理に伴いサンプル容量が1mL以上となるため，濃縮処理が必要である．

③②を逆相HPLCで25～40分画に分画．

④③の凍結乾燥物を，SDS-PAGEまたは二次元電気泳動を用いて比較分析．

この手法で12種類の高存在量タンパク質除去カラムと，一度に500 μg以上のタンパク質が分析できるアガロース二次元電気泳動法[6]を使った場合，300 μLの血清からスタートして，クマシー染色で100 ng/mL程度，蛍光検出で数ng/mL程度のタンパク質が検出可能である．

3 研究例

ここでは，DS法の抽出効率，DS法を起点とした比較分析法に関する基礎的なデータを示すとともに，大腸がん患者血清からバイオマーカー候補ペプチドを検出・同定した例を示す．

1）DS法の抽出効率と比較分析法の再現性

図1に，血清中のペプチドをDS法，有機溶媒沈殿法[7]（A法），限外濾過法[8]（F法）で抽出した成分を低分子用電気泳動法（Tricine-SDS-PAGE[9]）で分離し，比較した結果を示す．A法（レーン5），F法（レーン6，7）ではアルブミンをはじめとした高分子量タンパク質の除去に伴い，ペプチド成分の大部分が除去されているが，DS法（レーン3，4）では，高分子量タンパク質は若干残っているが分子量約20,000以下（点線内）のペプチド成分が他に比べて明らかに効率よく抽出されていることがわかる．また，矢印（←）で示した3種類のペプチドは血清

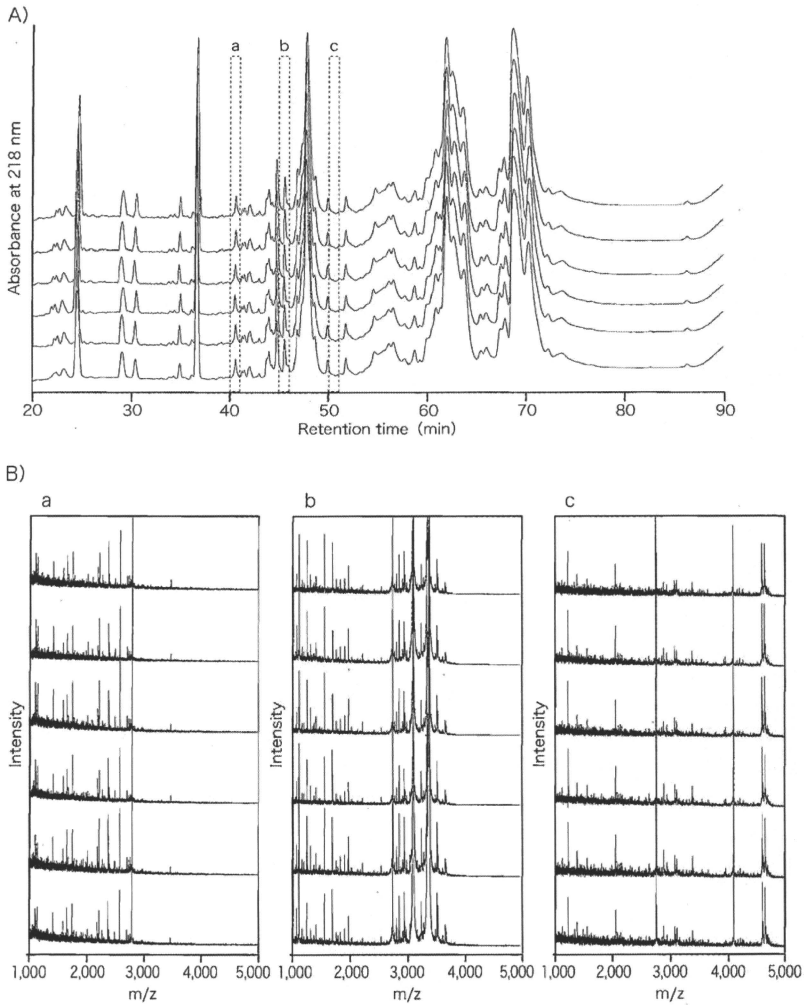

図2　DS法を基盤とした比較分析法の再現性

A）同質な血清6サンプル（各10μL）からDS法にて抽出したペプチドを逆相HPLC分析した結果．B）A）の溶出時間40～41分（a），45～46分（b），50～51分（c）における溶出物をMALDI-TOF-MS分析した結果．DS法は全過程を通して非常に再現性が高いことがわかる（文献4より転載）

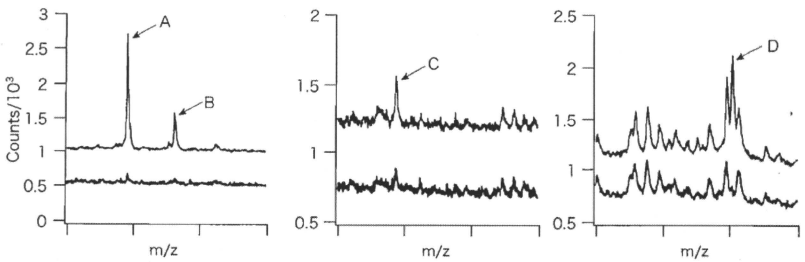

図3　大腸がんマーカー候補ペプチドの分析結果

概略図のペプチド比較分析法を用いて測定した大腸がん患者血清8例，健常者血清8例のMALDI-TOF-MSスペクトルの平均スペクトル．上側のスペクトルが大腸がん患者血清，下側のスペクトルが健常者血清である．また，A～Dは大腸がん診断マーカー候補ペプチドを示している（文献4より転載）

中の存在量が多いにもかかわらず，A法，F法ではその一部しか抽出できていないことがわかる．

複雑なペプチド混合物の中の微量成分を精度よく比較分析するためには，損失を抑えて細かく分画する必要がある．そこで，分画条件，分離カラムを検討し，逆相カラムにより60分画する方法を確立した．**図2A**に1種類の血清を6つに分けて，各10 μL中のペプチドをDS法で独立に抽出し，逆相HPLCで分析したクロマトグラフを示す．汎用タイプの逆相HPLCを使用し，溶媒流速を100 μL/minで使用しているため，非常に再現性よく分離できていることがわかる．**図2B**に60分画中の3分画（**図2A**中の溶出時間：a，b，c）のMALDI-TOF-MS測定結果を示す．この結果より，われわれのマーカーペプチド探索のための比較分析法は，全過程を通して非常に再現性が高いことがわかる．また，別の実験で健常者4例についてHPLCの60分画すべてについて分子量1,000～10,000を分析した結果，平均して約1,600種類のペプチドが検出され，そのうち約9割が4例中3例において強度1.5倍～1/2倍の範囲で観測されており，7割が4例中すべてにおいて同様に観測されていた（data not shown）．これだけ高い再現性で分析すると，予想以上に個人差が少なく，疾患に伴うペプチド組成の変化を系統的に分析できる可能性があることがわかる．

2）大腸がんマーカー候補ペプチドの探索

この方法を用いて大腸がん患者血清8例，健常者血清8例を比較分析した結果，4種類の大腸がん診断マーカー候補ペプチドの探索に成功した．**図3**に健常者血清8例ならびにがん患者血清8例のMSスペクトルの平均スペクトルを示す．A～Dのペプチドピークが大腸がん患者特異的に増加していることが明確にわかる．また，これらの4ピーク以外の部分が両方のスペクトルで非常によく一致している．このことは，われわれのマーカーペプチド探索法の精度が非常に高いことを示している．4種類のペプチドの大腸がんとの相関を示すP値はそれぞれ0.0013（A），0.0021（B），0.0006（C），0.0047（D）であった．また，一患者の血清に安定同位体標識ペプチドをDS法抽出前の血清に添加して同様の前処理の後にMALDI-TOF-MS分析した結果，A，Dについては数10～100 ng/mL，B，Cについては数ng/mLであった．これらのペプチドは他の方法を用いた研究においても血清中での報告例がなく，4種類中の1種類はがん細胞中で増加する細胞膜の裏

打ちタンパク質zyxinの部分ペプチドであることが判明した．以上の成果の詳細は参考文献[4]に記載しているので，参考にしていただきたい．

以上，血清16検体をDS法で処理しMALDI-TOF-MSでの測定およびデータ解析までの一連の操作を行うのに約3カ月の時間を要するが，そのほとんどがMALDI-TOF-MS測定とデータ解析に費やされており，DS法そのものの処理は約5時間で終了する．したがって，MALDI-TOF-MSの代わりにLC-MSで測定し，データ解析を専用ソフトを用いて行うなどの工夫をすることにより，スループットの格段の向上が期待できる．また，Three-step法に関しては，現在のところ血清8検体を二次元電気泳動で比較分析するために数週間を要している．

4 展望

●バイオマーカー候補タンパク質・ペプチドの臨床応用に向けた今後の課題

探索で見つかったバイオマーカー候補ペプチドの臨床応用を考える場合，ハイスループットな検証法を確立する必要がある．通常は抗体を用いたELISA系を使用したハイスループット定量解析を行うところであるが，ペプチドは多くがタンパク質の断片であるため，その断片だけを特異的に認識する抗体の作製が困難である．このため，バイオマーカー候補ペプチドの検証を行うためには抗体を用いない手法の確立が必須である．

近年，三連四重極型質量分析計を用いたSRM (Selected Reaction Monitoring) /MRM (Multiple Reaction Monitoring) 法によって，ペプチドを非常に感度よく，正確に定量できることがわかってきた．この手法により，血清・血漿中の微量なペプチドも検出できる可能性があると思われるが，感度を向上させるためにはこれまで述べてきた前処理法が欠かせないことは同じである．したがって，われわれが開発したDS法とSRM/MRM法を組み合わせることによって，より高感度な血清・血漿バイオマーカーペプチドの発見に貢献できると考えている．また，タンパク質分析全般に関しては，高存在量タンパク質の除去に多くの労力・時間とコストを要するだけでなく，高存在量タンパク質に結合した成分の分析が一部の方法を除いてはできていないのが現状である．この点では，難しい要求ではあるが，簡便で効果的な血清の分画法ならびに高存在量タンパク質除去法の開発が待たれるところである．

文献

1）Hiratsuka, S. et al. : Nat. Cell Biol., 8 : 1369-1375, 2006
2）Anderson, N. L. & Anderson, N. G : Mol. Cell. Proteomics, 1 : 845-867, 2002
3）Lai, K. K. Y. et al. : Hepatology, 47 : 1043-1051, 2008
4）Kawashima, Y. et al. : J. Proteome Res., 9 : 1694-1705, 2010
5）Kawashima, Y. et al. : J. Electrophoresis, 57 : 13-18, 2009
6）Oh-Ishi, M. & Maeda, T. : J. Chromatogr. B. Analyt. Technol. Biomed. Life Sci., 771 : 49-66, 2002
7）Chertov, O. et al. : Proteomics, 4 : 1195-1203, 2004
8）Tirumalai, R. S. et al. : Mol. Cell. Proteomics, 2 : 1096-1103, 2003
9）Schagger, H. et al. : Anal. Biochem., 166 : 368-379, 1987

Biomaterials 32 (2011) 162–169

Contents lists available at ScienceDirect

Biomaterials

journal homepage: www.elsevier.com/locate/biomaterials

Development of an antibody proteomics system using a phage antibody library for efficient screening of biomarker proteins

Sunao Imai [a,1], Kazuya Nagano [a,1], Yasunobu Yoshida [a], Takayuki Okamura [a], Takuya Yamashita [a,b], Yasuhiro Abe [a], Tomoaki Yoshikawa [a,b], Yasuo Yoshioka [a,b,c], Haruhiko Kamada [a,c], Yohei Mukai [a,b], Shinsaku Nakagawa [b,c], Yasuo Tsutsumi [a,b,c], Shin-ichi Tsunoda [a,b,c,*]

[a] Laboratory of Biopharmaceutical Research, National Institute of Biomedical Innovation, 7-6-8 Saito-Asagi, Ibaraki, Osaka 567-0085, Japan
[b] Graduate School of Pharmaceutical Sciences, Osaka University, 1-6 Yamadaoka, Suita, Osaka 565-0871, Japan
[c] The Center of Advanced Medical Engineering and informatics, Osaka University, 1-6 Yamadaoka, Suita, Osaka 565-0871, Japan

ARTICLE INFO

Article history:
Received 27 August 2010
Accepted 14 September 2010
Available online 8 October 2010

Keywords:
Protein
Image analysis
Immunochemistry
Molecular biology
Antibody
Cancer

ABSTRACT

Proteomics-based analysis is currently the most promising approach for identifying biomarker proteins for use in drug development. However, many candidate biomarker proteins that are over- or under-expressed in diseased tissues are found by such a procedure. Thus, establishment of an efficient method for screening and validating the more valuable targets is urgently required. Here, we describe the development of an "antibody proteomics system" that facilitates the screening of biomarker proteins from many candidates by rapid preparation of cross-reacting antibodies using phage antibody library technology. Using two-dimensional differential in-gel electrophoresis analysis, 16 over-expressed proteins from breast cancer cells were identified. Specifically, proteins were recovered from the gel pieces and a portion of each sample was used for mass spectrometry analysis. The remainder was immobilized onto a nitrocellulose membrane for antibody-expressing phage enrichment and selection. Using this procedure, antibody-expressing phages against each protein were successfully isolated within two weeks. The expression profiles of the identified proteins were then acquired by immunostaining of breast tumor tissue microarrays with the antibody-expressing phages. Using this approach, expression of Eph receptor A10, TRAIL-R2 and Cytokeratin 8 in breast tumor tissues were successfully validated.

These results demonstrate the antibody proteomics system is an efficient method for screening tumor-related biomarker proteins.

1. Introduction

Proteomics-based analysis is the most promising approach for identifying tumor-related biomarker proteins used in the drug development process [1–3]. The technological development of proteomics to seek and identify differentially expressed proteins in disease samples is expanding rapidly. However, in spite of the identification of many candidate biomarkers, the number of biomarker proteins successfully applied to drug development has been limited. The main difficulty is the lack of a methodology to comprehensively analyze the expression or function of many candidate proteins and to efficiently select potential biomarker proteins of interest. To circumvent this problem, an improved technology to efficiently screen the truly valuable proteins from a large number of candidates is desirable.

Monoclonal antibodies are extremely useful tools for the functional and distributional analysis of proteins [4–6]. For example, they can be applied to the specific detection and study of proteins through various techniques including ELISA, Western blotting, fluorescent imaging and tissue microarray analysis (TMA). Of all these techniques, TMA is particularly valuable because it enables the analysis of clinical expression profiles of antigens from many clinical samples [7–11]. However, the common hybridoma-based antibody production is a laborious and time-consuming method. Thus, it is impractical to create antibodies against many differentially expressed proteins identified by proteomics technologies, such as two-dimensional differential in-gel electrophoresis (2D-DIGE) [12–15]. Furthermore, a relatively large amount of antigen (several milligrams) is necessary to produce an antibody (i.e., immunization of animals or screening of positive clones). The

* Corresponding author. Laboratory of Biopharmaceutical Research, National Institute of Biomedical Innovation, 7-6-8 Saito-Asagi, Ibaraki, Osaka 567-0085, Japan. Tel.: +81 72 641 9814; fax: +81 72 641 9817.
E-mail address: tsunoda@nibio.go.jp (S.-i. Tsunoda).
[1] These authors contributed equally to the work.

0142-9612/$ – see front matter © 2010 Elsevier Ltd. All rights reserved.
doi:10.1016/j.biomaterials.2010.09.030

production of protein on this scale often requires engineering the corresponding gene for heterologous expression, which may require some time to optimize. In this respect, phage antibody library technology is able to construct a large repertoire protein or peptide consisting of hundreds of millions of molecules. Monoclonal antibodies against target antigens are then rapidly obtained from the phage libraries displaying single chain fragment variable (scFv) antibodies *in vitro* [16–21].

However, the amount of protein in spots detected by 2D-DIGE analysis is generally very small (hundreds of nanograms). Therefore, a technology for generating monoclonal antibodies from such small amounts of antigen needs to be developed. There are no reports that describe the successful isolation of antibodies against small amounts of proteins obtained from differential proteome analysis.

Here, we report the establishment of a method for the efficient isolation of scFv antibody-expressing phages from a small amount of protein antigen prepared *via* 2D-DIGE spots using a high quality non-immune mouse scFv phage library [22]. We also describe an efficient method for screening and validating tumor-related biomarker proteins of interest from a number of differentially expressed proteins by expression profiling using TMA and scFv antibody-expressing phages.

2. Materials and methods

2.1. Non-immune mouse scFv phage library

Construction of the improved non-immune murine scFv phage library has been described previously [22]. The phage library was prepared from a TG1 glycerol stock containing the scFv gene library.

2.2. Affinity panning using BIAcore® and nitrocellulose membrane

Three different amounts (5000 ng, 50 ng or 0.5 ng) of KDR-Fc chimera (R&D systems Inc., Minneapolis, MN) or a portion of the proteins (1–5 ng) extracted from 2D-DIGE spots were immobilized on a BIAcore sensor chip CM3® (BIAcore, Uppsala, Sweden) or on a nitrocellulose membrane. BIAcore-based panning has been described previously [22]. Membrane-based panning was performed using the Bio-Dot Microfiltration Apparatus (Bio-Rad Laboratories, Hercules, CA). The membrane was incubated with blocking solution (10% skimmed milk, 25% glycerol) for 2 h and then washed twice with 0.1% TBST (Tris-buffered saline containing 0.1% Tween 20). The model phage library (anti-KDR scFv antibody-expressing phages: wild type phage = 1: 100) or the non-immune scFv phage library was pre-incubated with 90% blocking solution at 4 °C for 1 h and then applied to each well. After 2–3 h incubation, the apparatus was washed ten times with TBST. Bound scFv antibody-expressing phages were then eluted with 100 mM triethylamine. The eluted phages were incubated in log phase *E. coli* TG1 cells and glycerol-stocks prepared for further repeat panning cycles. Phage titer was measured by counting the number of infected colony cells on Petrifilm (3M Co., St. Paul, MN).

2.3. Colony direct PCR

After the panning, colonies of phage-infected TG1 were picked up at random as PCR templates. The gene inserts of 16 clones were amplified by PCR using the following primers: primer-156 (5′-CAACGTGAAAAAATTATTATTCGC-3′) and primer-158 (5′-GTAAATGA ATTTTCTGTATGAGG-3′), which anneal to the sequences of pCANTAB5E phagemid vector (GE Healthcare Biosciences AB, Uppsala, Sweden). The size of insert DNA sequence was analyzed by agarose gel electrophoresis.

2.4. Cell lines

Human mammary gland cell line 184A1 (American Type Culture Collection; ATCC, Manassas, VA) was maintained by MEGM Bullet Kit (Takara Bio, Shiga, JAPAN). Mammary gland-derived breast cancer cell line SKBR3 (ATCC) was maintained in McCoy's 5a plus 10% FBS. All cells were grown at 37 °C in a humidified incubator with 5% CO_2.

2.5. 2D-DIGE analysis

Cell lysates were prepared from human mammary gland cell line 184A1 and mammary gland-derived breast cancer cell line SKBR3, and then solubilized with 7 M urea, 2 M thiourea, 4% CHAPS and 10 mM Tris–HCl (pH 8.5). The lysates were labeled at the ratio 50 μg protein: 400 pmol Cy3 or Cy5 protein labeling dye (GE Healthcare Biosciences AB) in dimethylformamide according to the manufacture's protocol. For first dimension separation, the labeled samples (each 50 μg) were combined and mixed with rehydration buffer (7 M urea, 2 M thiourea, 4% CHAPS, 2% DTT, 2% Pharmalyte (GE Healthcare Biosciences AB)) and applied to a 24-cm immobilized pH gradient gel strip (IPG-strip pH 5–6 NL). The samples for the spot-picking gel were prepared without labelling by Cy-dyes. For the second dimension separation, the IPG-strips were applied to SDS-PAGE gels (10% polyacrylamide and 2.7% N,N′-diallyltartardiamide gels). After electrophoresis, the gels were scanned with a laser fluoroimager (Typhoon Trio, GE Healthcare Biosciences AB). The spot-picking gel was scanned after staining with Flamingo solution (Bio-Rad). Quantitative analysis of protein spots was carried out with Decyder-DIA software (GE Healthcare Biosciences AB). For the antigen spots of interest, spots of 1 × 1 mm in size were picked using an Ettan Spot Picker (GE Healthcare Biosciences AB). Proteins were extracted by solubilizing the picked gel pieces using 88 mM sodium periodide. Protein volumes were determined by BSA standard in Colloid Gold Total Protein staining (Bio-Rad).

2.6. In-gel tryptic digestion

Spots of 1 mm × 1 mm in size were picked using an Ettan Spot Picker and digested with trypsin as described below. The gel pieces were then destained with 50% acetonitrile/50 mM NH_4HCO_3 for 20 min twice, dehydrated with 75% acetonitrile for 20 min, and then dried using a centrifugal concentrator. Next, 5 μl of 20 μl/ml trypsin (Promega, Madison, WI) solution was added to each gel piece and incubated for 16 h at 37 °C. Three solutions were used to extract the resulting peptide mixtures from the gel pieces. First, 50 μl of 50% (v/v) acetonitrile in 1% (v/v) aqueous trifluoroacetic acid (TFA) was added to the gel pieces, which were then sonicated for 5 min. Next, we collected the solution and added 80% (v/v) acetonitrile in 0.2% TFA. Finally, 100% acetonitrile was added for the last extraction. The peptides were dried and then resuspended in 10 μl of 0.1% TFA before being cleaned using ZipTip^{TM} μC_{18} pipette tips (Millipore, Billerica, MA). The tips were wetted with three washes in 50% acetonitrile and equilibrated with three washes in 0.1% TFA, then the peptides were aspirated 10 times to ensure binding to the column. The column and peptides were washed three times in 0.1% TFA before being eluted in 1 μl of 80% acetonitrile/0.2% TFA.

2.7. Mass spectrometry (MS) and database search

The tryptic digests (0.6 μl) were mixed with 0.6 μl α-cyano-4-hydroxy-trans-cinnamic acid saturated in a 0.1% TFA and acetonitrile solution (1:1vol/vol). Each mixture was deposited onto a well of a 96-well target plate and then analyzed by matrix-assisted laser desorption ionization time-of-flight mass spectrometry (MALDI-TOF/MS; autoflexII, Bruker Daltonics, Billerica, WI) in the Reflectron mode. The mass axis was adjusted with calibration peptide (BRUKER DALTNICS) peaks (M/z 1047.19, 1296.68, or 2465.19) as lock masses. Bioinformatic databases were searched to identify the proteins based on the tryptic fragment sizes. The Mascot search engine (http://www.matrixscience.com) was initially used to query the entire theoretical tryptic peptide as well as SwissProt (http://www.expasy.org/, a public domain database provided by the Swiss Institute of Bioinformatics, Geneva, Switzerland). The search query assumed the following: (i) the peptides were monoisotopic (ii) methionine residues may be oxidized (iii) all cysteines are modified with iodoacetamide.

2.8. Phage ELISA using nitrocellulose membrane

Phage ELISA using scFv antibody-expressing phages was performed as previously described [22]. Briefly, phage-infected TG1 clones were picked, monocloned in a Bio-Dot Microfiltration Apparatus and scFv antibody-expressing phages propagated. The supernatants containing scFv antibody-expressing phages were incubated with immobilized proteins (~1 ng) extracted from 2D-DIGE spots. scFv antibody-expressing phages bound to 2D-DIGE spots were visualized using HRP-conjugated anti-M13 monoclonal antibody (GE Healthcare Biosciences AB).

2.9. Immunohistochemical staining using scFv antibody-expressing phages

Human breast cancer and normal TMA (Super Bio Chips, Seoul, South Korea & Biomax, Rockville, MD) were deparaffinated in xylene and rehydrated in a graded series of ethanol. Heat-induced epitope retrieval was performed in while keeping Target Retrieval Solution pH 9 (Dako, Glostrup, Denmark) temperature following the manufacturer's instructions. Heat-induced epitope retrieval was performed while maintaining the Target Retrieval Solution pH 9 (Dako) at the desired temperature according to the manufacturer's instructions. After heat-induced epitope retrieval treatment, endogenous peroxidase was blocked with 0.3% H_2O_2 in TBS for 5 min followed by washing twice in TBS. TMA were incubated with 5% BSA blocking solution for 15 min. The slides were then incubated with the primary scFv antibody-expressing phages (10^{12} CFU/ml) for 60 min. After washing three times with 0.05% TBST, each series of sections was incubated for 30 min with ENVISION + Dual Link (Dako), washed three times in TBST. The reaction products were rinsed twice with TBST, and then developed in liquid 3,3′-diaminobenzidine (Dako) for 3 min. After the development, sections were washed twice with distilled water, lightly

counterstained with Mayer's hematoxylin, dehydrated, cleared, and mounted with resinous mounting medium. All procedures were performed using AutoStainer (Dako).

2.10. TMA Immunohistochemistry scoring

The optimized staining condition for breast tumor tissue microarray was determined based on the coexistence of both positive and negative cells in the same tissue sample. Signals were considered positive when reaction products were localized in the expected cellular component. The criteria for the staining were scored as follows: distribution score was scored as 0 (0%), 1 (1–50%), and 2 (51–100%) to indicate the percentage of positive cells in all tumor cells present in one tissue. The intensity of the signal (intensity score) was scored as 0 (no signal), 1 (weak), 2 (moderate) or 3 (marked). The total of the distribution score and intensity score was then summed into a total score (TS) of TS0 (sum = 0), TS1 (sum = 2), TS2 (sum = 3), and TS3 (sum = 4–5). Throughout this study, TS0 or TS1 was regarded as negative, whereas TS2 or TS3 was regarded as positive. Statview software was used in statistical analysis.

3. Results

3.1. Optimization of panning methods

To establish a method for the efficient isolation of antibodies against a small amount of protein antigen (nanogram-order or less) prepared from 2D-DIGE spots, 5000 ng, 50 ng or 0.5 ng of recombinant KDR proteins were first immobilized on a BIAcore sensor chip CM3® or on a nitrocellulose membrane using the Bio-Dot Microfiltration Apparatus®. Isolation of antibodies was assessed using a model phage library (anti-KDR scFv antibody-expressing phages: wild type phage = 1: 100) (Fig. 1). Enrichment of the desired clones in the output library was evaluated by analyzing the gene inserts of randomly-picked phage-infected TG1 cells by colony direct PCR. In the method using BIAcore®, enrichment was observed when 5000 ng of KDR was used for immobilization. By contrast, Membrane-based panning led to the successful enrichment of anti-KDR scFv antibodies from only 0.5 ng of KDR. These results demonstrated that membrane-based panning was suitable for the isolation of antibodies from very small amounts of antigen extracted from 2D-DIGE spot gel pieces.

3.2. 2D-DIGE analysis and identification of differentially expressed proteins

To identify breast tumor-related biomarker proteins and isolate monoclonal antibodies against them, we performed 2D-DIGE using breast cancer cell lines SKBR3 and normal breast cell lines 184A1 (Fig. 2). Quantitative analysis showed that 21 spots displayed increased or decreased expression levels in the cancer cell line compared with the normal cell line. MALDI-TOF/MS analysis of the spots subsequently identified 16 different proteins (Table 1).

3.3. Isolation of antibodies against each 2D-DIGE spot from the non-immune scFv phage library

The amount of protein extracted from the gel pieces ranged from several tens of nanogram to a few micrograms (Table 1). Because the membrane-based panning method facilitates the isolation of antibodies from 0.5 ng of protein (Fig. 1), we reasoned that this method could be used to isolate antibodies from the small amounts of proteins extracted from 2D-DIGE spot gel pieces. Thus a portion of the extracted proteins were immobilized onto nitrocellulose membranes by means of a Bio-Dot Microfiltration Apparatus, and membrane-based panning was performed using the non-immune scFv phage library [22] (Table 2). The results from this panning showed that the output/input ratio of phage titer (titer of the recovered phage library after the panning/titer of phage library before the panning) after the fourth round of panning against all spots increased approximately 20-fold–4000-fold in comparison to that obtained from the first round of panning. This elevated output/input ratio indicated the enrichment of the antigen-binding scFv antibody clones. To isolate monoclonal scFv antibodies to each spot, a total of 60 clones were randomly picked from the 4th panning output phage library and binding of the monoclonal scFv antibody-expressing phages to each antigen was tested by phage ELISA. As a result, several scFv antibody clones binding to each of the 16 antigens were isolated (Table 2). The antigenic specificity of isolated scFv antibodies was investigated by dot blot using various proteins as antigens. Some of the isolated scFv antibodies bound specifically to the antigen protein, but not to the His-tagged caspase-8, His-tagged importin-β, tumor necrosis factor receptor 1 (TNFR1)-Fc-chimera and KDR-Fc-chimera (data not shown). These results indicated the successful isolation of each spot-specific scFv antibody-expressing phages after only two weeks.

3.4. TMA analysis

The next stage in the process was to select the most valuable breast tumor-related biomarker proteins from a large number of

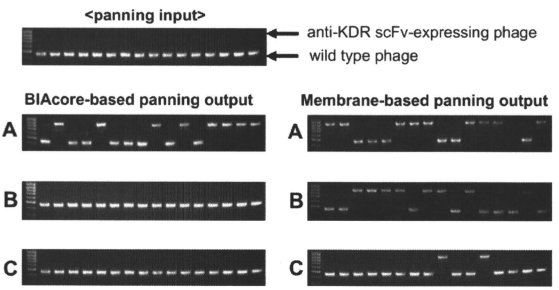

Fig. 1. Optimization of panning methods to isolate monoclonal antibodies from a very small amount of antigen. Model panning was performed using the BIAcore® or nitrocellulose membrane. The model library (anti-KDR scFv phage : wild type phage = 1: 100) was incubated with KDR ((A) 5000 ng, (B) 50 ng, (C) 0.5 ng) immobilized on a sensor chip or nitrocellulose membrane. The BIAcore-based panning method has been previously described [22]. After the binding step, the nitrocellulose membrane was washed ten times with TBST. The bound scFv antibody-expressing phages were eluted with triethylamine. The eluted scFv antibody-expressing phages were then incubated in log phase TG1 cells and individual TG1 clones were picked at random. Inserts of 16 phage clones were amplified by PCR. The gene sizes of inserts were analyzed by agarose gel electrophoresis.

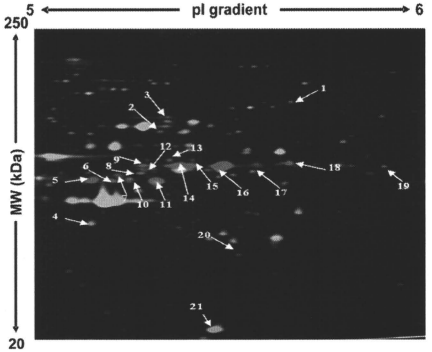

Fig. 2. 2D-DIGE image of fluorescently labeled proteins from SKBR3 and 184A cell. Breast cancer cell line (SKBR3) and normal breast cell line (184A1) were labeled using cy3 and cy5, respectively. The protein samples were then subjected to 2D electrophoresis. Spots that were over- and under-expressed in mammary cancer cells relative to normal cells were colored red and green, respectively. Yellow color spots show no change in expression.

identified candidate proteins. To this end, we immunostained TMA slides with 189 cases of breast tumors and 15 cases of normal breast specimens using the isolated spot-specific scFv antibody-expressing phages and screened the promising candidate biomarker proteins in terms of the expression profile in breast tumor tissues and normal tissues (Table 3). The result of the expression profile analysis showed that SPATA5, beta-actin variant, FLJ31438, PAK65, XRN1 and Jerky protein homolog-like were not expressed in normal and breast cancer tissue at all. By contrast, TRAIL-R2, Cytokeratin 8 and Eph receptor A10 were highly and specifically expressed (Fig. 3) in 63, 73 and 49% of breast tumor cases respectively, while the existing-breast cancer marker, Her-2, was expressed in 28% of breast tumor cases (Table 3). Thus, the relationship between the expression of each antigen and the Her-2 expression profile was analyzed. The level of expression of TRAIL-R2, Cytokeratin 8 and Eph receptor A10 in Her-2 positive cases were 77, 77 and 62%, and in Her-2 negative cases were 57, 67 and 44%, respectively (Table 4). Furthermore, the relationship between the expression of each antigen and clinical stage was analyzed in 187 of the 189 cases where all the clinical data was available. The level of expression of Cytokeratin 8 and Eph receptor A10 increased with progression of clinical symptoms (Table 5).

Table 1
Identification of 2D-DIGE spots by MALDI-TOF/MS.

Spot	Protein name	Accession number	MW (kDa)	pI	Protein volume (ng)	Expression ratio [cancer/normal] (fold)
#1	splicing factor YT521-B	Q96MU7	85	5.9	119	6
#2	IkappaBR	Q96HA7	63	5.5	104	6
#3	SPATA5	C9JT97	76	5.6	94	7
#4	skin aspartic protease	Q53RT3	37	5.3	610	0.1
#5	beta actin variant	P60709	42	5.3	99	15
#6	TRAIL-R2	O14763	48	5.4	100	18
#7	Cytokeratin-18	P05783	48	5.3	99	12
#8	TRAIL-R2	O14763	48	5.4	95	16
#9	RREB1	Q92766	52	5.3	109	10
#10	Cytokeratin-7	P08729	51	5.4	126	23
#11	Cytokeratin-18	P05783	48	5.3	497	13
#12	Cytokeratin-7	P08729	51	5.4	122	24
#13	FLJ31438	Q96N41	53	5.5	126	35
#14	Cytokeratin-7	P08729	51	5.4	406	36
#15	PAK65	Q13177	55	5.7	677	8
#16	Cytokeratin 8	P05787	54	5.5	694	32
#17	Cytokeratin 8	P05787	54	5.5	1143	72
#18	XRN1	Q8IZH2	54	5.8	353	8
#19	Jerky protein homolog-like	Q9Y4A0	51	6.0	130	22
#20	Eph receptor A10	Q5JZY3	32	5.7	119	9
#21	Glutathione S-transferase P	P09211	23	5.4	119	0.02

Table 2
Enrichment and isolation of antibodies to 2D-DIGE spots from non-immune libraries.

Spot	Protein name	Output/Input Ratio ($\times 10^{-7}$)/round				The number of isolated mAb.
		1st	2nd	3rd	4th	
#1	splicing factor YT521-B	6	7	16	480	4
#2	IkappaBR	6	7	15	500	3
#3	SPATA5	5	6	32	860	2
#4	skin aspartic protease	5	6	5	24	1
#5	beta actin variant	7	11	17	480	1
#6	TRAIL-R2	6	7	25	420	5
#7	Cytokeratin 18	5	11	62	260	4
#8	TRAIL-R2	5	27	41	1500	5
#9	RREB1	8	9	14	370	7
#10	Cytokeratin 7	6	7	3	2200	5
#11	Cytokeratin 18	6	8	15	84	2
#12	Cytokeratin 7	10	11	13	94	2
#13	FLJ31438	7	9	32	80	6
#14	Cytokeratin 7	4	7	46	280	5
#15	PAK65	7	11	51	580	9
#16	Cytokeratin 8	8	7	16	4100	6
#17	Cytokeratin 8	5	12	33	240	2
#18	XRN1	6	20	18	200	1
#19	Jerky protein homolog-like	7	10	49	940	3
#20	Eph receptor A10	8	6	57	3000	2
#21	Glutathione S-transferase P	7	8	110	1900	2

4. Discussion

Here, we aimed to develop a method of efficiently screening tumor-related biomarker proteins by proteome analysis. In

Table 3
Positive rate of identified proteins in breast cancer and normal breast tissues.

Protein name	Positive rate of antigens			
	Normal breast tissues		Breast cancer tissues	
Her-2	0/15	(0%)	53/189	(28%)
IkappaBR	3/15	(20%)	22/189	(12%)
SPATA5	0/15	(0%)	0/189	(0%)
beta actin variant	0/15	(0%)	0/189	(0%)
TRAIL-R2	0/15	(0%)	119/189	(63%)
RREB1	1/15	(7%)	83/189	(44%)
FLJ31438	0/15	(0%)	0/189	(0%)
PAK65	0/15	(0%)	0/189	(0%)
Cytokeratin 8	0/15	(0%)	137/189	(73%)
XRN1	0/15	(0%)	0/189	(0%)
Jerky protein homolog-like	0/15	(0%)	0/189	(0%)
Eph receptor A10	0/15	(0%)	93/189	(49%)

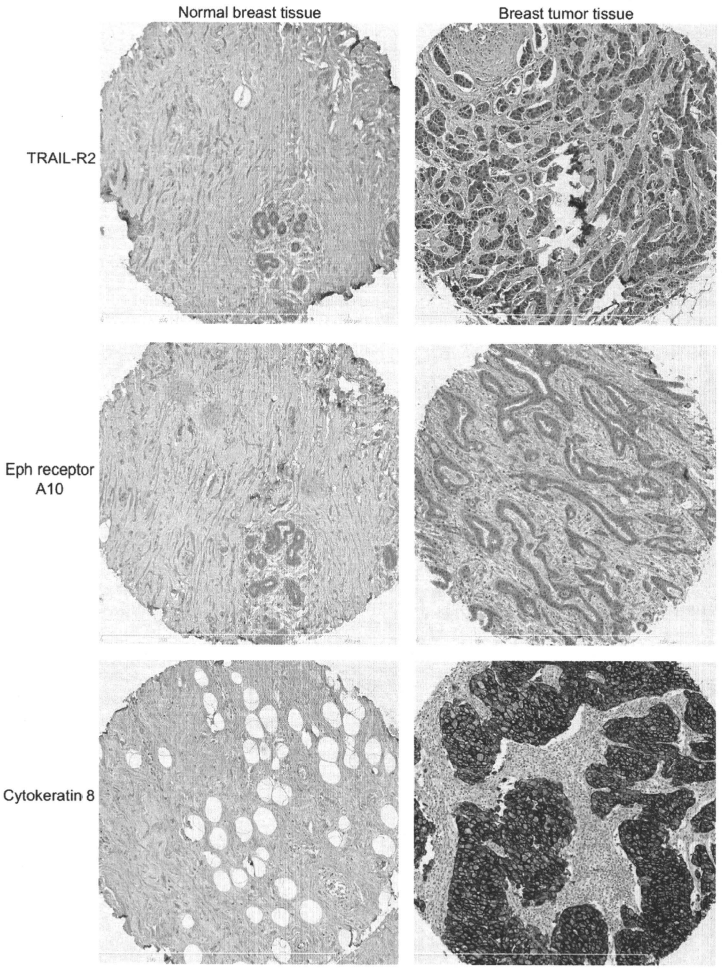

Fig. 3. Immunohistochemical staining of breast tumor and normal breast tissue microarray by scFv antibody-expressing phages. Typical images of breast cancer and normal breast tissue microarray stained by using scFv antibody-expressing phages to TRAIL-R2, Eph receptor A10 and Cytokeratin 8 are shown. Left panels are normal breast tissues and right panels are breast tumors. The tissue microarrays were counterstained by hematoxylin.

particular, we attempted to establish a means of isolating specific antibodies directly from small amounts of differentially expressed proteins obtained *via* 2D-DIGE analysis. To achieve this, we focused on a non-immune scFv phage library. Because the non-immune naïve scFv phage library has a huge repertoire of scFv on the surface of the phages, monoclonal antibodies to every antigen could be effectively isolated *in vitro*. Generally the diversity of the CDR3 domain, which is important for antigen-binding specificity, is estimated to be approximately twenty million [23]. Thus we reasoned that our previously constructed library, containing 2.4×10^9 scFv variants, has almost equal potential as the murine or human immune system [22]. Initially, in order to isolate monoclonal antibodies against very small amounts of antigen (hundreds of nanograms) recovered from the spots of 2D-DIGE analysis, we attempted to optimize the panning method using either a BIAcore® or nitrocellulose membrane. In the method using BIAcore®, the

Table 4
Positive rate of identified proteins in Her-2 positive and Her-2 negative cases.

Protein name	Positive rate of antigens in Her-2	
	Positive cases	Negative cases
TRAIL-R2	41/53 (77%)	78/136 (57%)
Cytokeratin 8	41/53 (77%)	91/136 (67%)
Eph receptor A10	33/53 (62%)	60/136 (44%)
TRAIL-R2 or Eph receptor A10	46/53 (87%)	100/136 (74%)

Table 5
Positive rate of identified proteins in clinical stage.

Protein name	Positive rate of antigens in clinical stage					
	Stage I		Stage II		Stage III	
Her-2	6/14	(43%)	17/87	(20%)	30/86	(35%)
TRAIL-R2	11/14	(79%)	51/87	(59%)	55/86	(64%)
Cytokeratin 8*	7/14	(50%)	58/87	(67%)	71/86	(83%)
Eph receptor A10*	4/14	(29%)	42/87	(48%)	47/86	(55%)

Man Whitney U test $^*P < 0.05$

enrichment of the desired clones was observed when immobilizing 5000 ng of KDR. By contrast, membrane-based panning led to the successful enrichment of clones from only 0.5 ng of KDR (Fig. 1). BIAcore-based panning has been recognized to be an effective method because the interaction of an antigen and a scFv antibody can be monitored in real time and the operation can be automated [24,25]. However, our results suggest that BIAcore® is inefficient for immobilizing very small amounts of antigen. This is because antigen immobilization using the BIAcore procedure requires a chemical coupling reaction with the surface of the sensor chip. In contrast, the membrane-based panning method is suitable for the isolation of antibodies against very small amounts of antigens. The suitability of this procedure when handling such small amounts of proteins presumably arises from the high efficiency of adsorption of antigens by the nitrocellulose membrane. These results show that monoclonal antibodies can be created from small amounts of proteins recovered from 2D-DIGE spots.

In breast cancer patients, the antibody targeting human epidermal growth factor receptor II (Her-2), is an effective drug [26,27]. However, because this receptor is over-expressed in only ~25% of breast cancer patients, anti-Her-2 antibody therapy is ineffective in ~75% of cases. Furthemore, approximately 30% of Her-2 over-expressed patients that received anti-Her-2 antibody therapy became tolerant [28–30]. Thus, we applied our antibody proteomics system to breast cancer samples for identification of the proteins to replace Her-2 as suitable therapeutic targets. Initially, 21 differentially expressed proteins between SKBR3 and 184A1 cells were found by 2D-DIGE analysis and 16 different proteins were identified by MALDI-TOF/MS. Four of the identified proteins were present in more than one spot i.e., TRAIL-R2 (spot 6, 8), Cytokeratin 18 (spot 7, 11), Cytokeratin 8 (spot 16, 17) and Cytokeratin 7 (spot 10, 12, 14). These proteins presumably display different pI and MW values due to posttranslational modification. Next, membrane-based panning against these spots was performed, and the output/input ratio of phage titer after the fourth round of panning increased from approximately 20-fold–4000-fold in comparison to that after the first round of panning. Moreover, we screened scFv antibody-expressing phages binding to each spot protein by phage ELISA and obtained each spot-specific scFv antibodies from all spots after approximately two weeks. Finally, it was necessary to select the most valuable proteins from a large number of differentially expressed proteins in breast cancer cells. Using the isolated spot-specific scFv antibody-expressing phages, we immunostained a TMA with 189 cases of breast cancer tissue and 15 samples of normal tissue. SPATA5, Beta actin, FLJ31438, PAK65 and XRN1 were not detected in either the tumor tissue or normal tissue. Thus, these proteins may have been derived from cell lines used in the

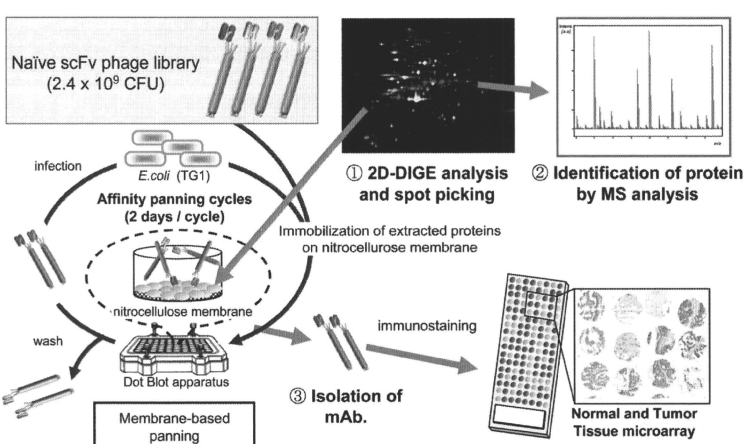

Fig. 4. Schematic illustration of the antibody proteomics system. Antibody proteomics system is an efficient method for screening tumor-related biomarker proteins. Because this system involves the direct isolation of monoclonal antibodies from 2D-DIGE spots without preparation of recombinant proteins, it enables the discovery and validation of tumor-related biomarker proteins by TMA analysis using the isolated scFv antibody-expressing phages.

proteome analysis or the antibodies against these proteins may not detect the antigen on formalin-fixed paraffin-embedded tissues. By contrast, TRAIL-R2, Cytokeratin 8 and Eph receptor A10 were specifically-expressed in over 40% of breast cancer tissues. We confirmed the immunohistochemical staining image generated by scFv antibody-expressing phages displayed a similar pattern to that generated by IgG type commercial antibody (data not shown). Interestingly, the expression rates of TRAIL-R2, Cytokeratin 8 and Eph receptor A10 were higher than the existing breast cancer marker, Her-2 (only about 25%). Moreover, the expression rates of TRAIL-R2 and Eph receptor A10 (cell membrane proteins) in Her-2 negative cases were over 40% and in Her-2 positive cases over 60%. This data indicates that TRAIL-R2 and Eph receptor A10 are promising alternative target candidates for anti-Her-2 antibody therapy ineffective patients, at least in terms of the expression profile. Further work is required to analyze the function of these proteins in more detail. Furthermore, by checking antigen expression profiles against clinical information, the expression rate of Cytokeratin 8 and Eph receptor A10 was found to have increased during progression of the clinical symptoms. These observations indicate that Cytokeratin 8 and Eph receptor A10 are promising diagnostic marker candidates for assessing the aggressiveness of breast cancer.

Recently, an anti-TRAIL-R2 antibody has been developed as an anticancer drug [31–33]. Moreover, Cytokeratin 8 has gained considerable attention as a cancer aggressiveness diagnostic marker [34–36]. These results demonstrate that this technology is able to select well-known drug-target markers (i.e., TRAIL-R2) and diagnostic markers (i.e., Cytokeratin 8) as well as unknown biomarker protein candidates (Eph receptor A10) from a large variety of differentially expressed proteins in cancer cells.

Our method employs a set of techniques for efficiently identifying biomarker candidates. Specifically, the method entails; 1) searching for differentially expressed proteins in disease samples, 2) identification of the proteins, 3) high throughput isolation of monoclonal antibodies against the proteins using a naïve scFv phage library, and 4) validation of the proteins by TMA analysis. This methodology is referred to as an "antibody proteomics system" (Fig. 4). We believe that the proteins identified using this approach will contribute to the drug development process. Indeed, the antibody proteomics system could become a platform technology for seeking tumor-related biomarker proteins by a proteomics-based approach.

5. Conclusions

In this study, we established the antibody proteomics system for efficiently screening and validating tumor-related biomarker proteins of interest by isolating specific antibodies directly from small amounts of proteins obtained *via* 2D-DIGE analysis. Applying this technique to the identification of breast tumor-related biomarker proteins, the expressions of Eph receptor A10, TRAIL-R2 and Cytokeratin 8 in breast tumor tissues were successfully validated from a large number of candidates. These results demonstrate that our original technology is an efficient and useful method for screening tumor-related biomarker proteins. Moreover, Eph receptor A10, TRAIL-R2 and Cytokeratin 8 identified in this study are promising breast tumor biomarkers for drug development.

Acknowledgement

We thank Dr. Junya Fukuoka, Department of Surgical Pathology, Toyama University Hospital, for valuable advice during our pathological analysis.

This study was supported in part by Grants-in-Aid for Scientific Research from the Ministry of Education, Culture, Sports, Science and Technology of Japan, and from the Japan Society for the Promotion of Science (JSPS). This study was also supported in part by Health Labour Sciences Research Grants from the Ministry of Health, Labor and Welfare of Japan, and by Health Sciences Research Grants for Research on Publicly Essential Drugs and Medical Devices from the Japan Health Sciences Foundation.

Appendix

Figure with essential color discrimination. Figs. 2–4 in this article have parts that are difficult to interpret in black and white. The full color images can be found in the on-line version, at doi:10.1016/j.biomaterials.2010.09.030.

References

[1] Hanash S. Disease proteomics. Nature 2003;422(6928):226–32.
[2] Kavallaris M, Marshall GM. Proteomics and disease: opportunities and challenges. Med J Aust 2005;182(11):575–9.
[3] Oh-Ishi M, Maeda T. Disease proteomics of high-molecular-mass proteins by two-dimensional gel electrophoresis with agarose gels in the first dimension (Agarose 2-DE). J Chromatogr B Analyt Technol Biomed Life Sci 2007;849 (1–2):211–22.
[4] Chaga GS. Antibody arrays for determination of relative protein abundances. Methods Mol Biol 2008;441:129–51.
[5] Kaufmann H, Bailey JE, Fussenegger M. Use of antibodies for detection of phosphorylated proteins separated by two-dimensional gel electrophoresis. Proteomics 2001;1(2):194–9.
[6] Xu ZW, Zhang T, Song CJ, Li Q, Zhuang R, Yang K, et al. Application of sandwich ELISA for detecting tag fusion proteins in high throughput. Appl Microbiol Biotechnol 2008;81(1):183–9.
[7] Au NH, Gown AM, Cheang M, Huntsman D, Yorida E, Elliott WM, et al. P63 expression in lung carcinoma: a tissue microarray study of 408 cases. Appl Immunohistochem Mol Morphol 2004;12(3):240–7.
[8] de Jong D, Xie W, Rosenwald A, Chhanabhai M, Gaulard P, Klapper W, et al. Immunohistochemical prognostic markers in diffuse large B-cell lymphoma: validation of tissue microarray as a prerequisite for broad clinical applications (a study from the Lunenburg Lymphoma Biomarker Consortium). J Clin Pathol 2009;62(2):128–38.
[9] Kozarova A, Petrinac S, Ali A, Hudson JW. Array of informatics: applications in modern research. J Proteome Res 2006;5(5):1051–9.
[10] Rimm DL, Camp RL, Charette LA, Costa J, Olsen DA, Reiss M. Tissue microarray: a new technology for amplification of tissue resources. Cancer J 2001;7 (1):24–31.
[11] Tawfik El-Mansi M, Williams AR. Validation of tissue microarray technology using cervical adenocarcinoma and its precursors as a model system. Int J Gynecol Cancer 2006;16(3):1225–33.
[12] Asadi A, Pourfathollah AA, Mahdavi M, Eftekharian MM, Moazzeni SM. Preparation of antibody against horseradish peroxidase using hybridoma technology. Hum Antibodies 2008;17(3–4):73–8.
[13] Hadas E, Theilen G. Production of monoclonal antibodies. The effect of hybridoma concentration on the yield of antibody-producing clones. J Immunol Methods 1987;96(1):3–6.
[14] Makonkawkeyoon L, Pharephan S, Makonkawkeyoon S. Production of a mouse hybridoma secreting monoclonal antibody highly specific to hemoglobin Bart's (gamma4). Lab Hematol 2006;12(4):193–200.
[15] McKinney KL, Dilwith R, Belfort G. Optimizing antibody production in batch hybridoma cell culture. J Biotechnol 1995;40(1):31–48.
[16] Barbas 3rd CF, Kang AS, Lerner RA, Benkovic SJ. Assembly of combinatorial antibody libraries on phage surfaces: the gene III site. Proc Natl Acad Sci U S A 1991;88(18):7978–82.
[17] Coomber DW. Panning of antibody phage-display libraries. Standard protocols. Methods Mol Biol 2002;178:133–45.
[18] McCafferty J, Griffiths AD, Winter G, Chiswell DJ. Phage antibodies: filamentous phage displaying antibody variable domains. Nature 1990;348 (6301):552–4.
[19] Okamoto T, Mukai Y, Yoshioka Y, Shibata H, Kawamura M, Yamamoto Y, et al. Optimal construction of non-immune scFv phage display libraries from mouse bone marrow and spleen established to select specific scFvs efficiently binding to antigen. Biochem Biophys Res Commun 2004;323 (2):583–91.
[20] Smith GP. Filamentous fusion phage: novel expression vectors that display cloned antigens on the virion surface. Science 1985;228(4705):1315–7.
[21] Vaughan TJ, Williams AJ, Pritchard K, Osbourn JK, Pope AR, Earnshaw JC, et al. Human antibodies with sub-nanomolar affinities isolated from a large non-immunized phage display library. Nat Biotechnol 1996;14(3):309–14.

[22] Imai S, Mukai Y, Nagano K, Shibata H, Sugita T, Abe Y, et al. Quality enhancement of the non-immune phage scFv library to isolate effective antibodies. Biol Pharm Bull 2006;29(7):1325–30.
[23] Xu JL, Davis MM. Diversity in the CDR3 region of V(H) is sufficient for most antibody specificities. Immunity 2000;13(1):37–45.
[24] Schier R, Marks JD. Efficient in vitro affinity maturation of phage antibodies using BIAcore guided selections. Hum Antibodies Hybridomas 1996;7 (3):97–105.
[25] Sheets MD, Amersdorfer P, Finnern R, Sargent P, Lindquist E, Schier R, et al. Efficient construction of a large nonimmune phage antibody library: the production of high-affinity human single-chain antibodies to protein antigens. Proc Natl Acad Sci U S A 1998;95(11):6157–62.
[26] Baselga J, Norton L, Albanell J, Kim YM, Mendelsohn J. Recombinant humanized anti-HER2 antibody (Herceptin) enhances the antitumor activity of paclitaxel and doxorubicin against HER2/neu overexpressing human breast cancer xenografts. Cancer Res 1998;58(13):2825–31.
[27] Pietras RJ, Pegram MD, Finn RS, Maneval DA, Slamon DJ. Remission of human breast cancer xenografts on therapy with humanized monoclonal antibody to HER-2 receptor and DNA-reactive drugs. Oncogene 1998;17(17):2235–49.
[28] Amar S, Moreno-Aspitia A, Perez EA. Issues and controversies in the treatment of HER2 positive metastatic breast cancer. Breast Cancer Res Treat 2008;109(1):1–7.
[29] Nahta R, Esteva FJ. In vitro effects of trastuzumab and vinorelbine in trastuzumab-resistant breast cancer cells. Cancer Chemother Pharmacol 2004;53 (2):186–90.
[30] Nahta R, Yu D, Hung MC, Hortobagyi GN, Esteva FJ. Mechanisms of disease: understanding resistance to HER2-targeted therapy in human breast cancer. Nat Clin Pract Oncol 2006;3(5):269–80.
[31] Plummer R, Attard G, Pacey S, Li L, Razak A, Perrett R, et al. Phase 1 and pharmacokinetic study of lexatumumab in patients with advanced cancers. Clin Cancer Res 2007;13(20):6187–94.
[32] Tolcher AW, Mita M, Meropol NJ, von Mehren M, Patnaik A, Padavic K, et al. Phase I pharmacokinetic and biologic correlative study of mapatumumab, a fully human monoclonal antibody with agonist activity to tumor necrosis factor-related apoptosis-inducing ligand receptor-1. J Clin Oncol 2007;25 (11):1390–5.
[33] Vannucchi S, Chiantore MV, Fiorucci G, Percario ZA, Leone S, Affabris E, et al. TRAIL is a key target in S-phase slowing-dependent apoptosis induced by interferon-beta in cervical carcinoma cells. Oncogene 2005;24(15):2536–46.
[34] Ditzel HJ, Strik MC, Larsen MK, Willis AC, Waseem A, Kejling K, et al. Cancer-associated cleavage of cytokeratin 8/18 heterotypic complexes exposes a neoepitope in human adenocarcinomas. J Biol Chem 2002;277 (24):21712–22.
[35] Fukunaga Y, Bandoh S, Fujita J, Yang Y, Ueda Y, Hojo S, et al. Expression of cytokeratin 8 in lung cancer cell lines and measurement of serum cytokeratin 8 in lung cancer patients. Lung Cancer 2002;38(1):31–8.
[36] Wolff JM, Borchers H, Brehmer Jr B, Brauers A, Jakse G. Cytokeratin 8/18 levels in patients with prostate cancer and benign prostatic hyperplasia. Urol Int 1998;60(3):152–5.